TABLE IV. The table gives the values of $B(E2)$ and $G$ for transitions in $V^{51}$ and $Cr^{52}$ measured by other workers. Values of $G$ are given in brackets. The values of $G$ for the 0.930-MeV transition in $V^{51}$ compare favorably, for the most part, with the value 11.0 measured in the present experiment.

| | | | $B(E2)$ and $G$[a] | | | | |
|---|---|---|---|---|---|---|---|
| $\epsilon$ MeV | Nuclide | $B_T(E2)$ | Gove and Broude[b] | Adams *et al.*[b] | Lemberg[b] | Stelson[c] | McGowan *et al.*[d] |
| 0.320 | $V^{51}$ | 0.184 | 0.65<br>(3.53) | 0.60±0.15<br>(3.26±0.8) | | 0.65<br>3.53 | |
| 0.930 | $V^{51}$ | 0.043 | 0.19[e]<br>(4.4) | 0.40<br>(9.3) | 0.55<br>(12.1) | | |
| 1.43 | $Cr^{52}$ | 0.50 | | 3.0 ±0.75<br>(6.0 ±1.5) | 3.2±0.6<br>(6.4±1.2) | | 3.62±0.39<br>(7.25±0.8) |

[a] $B(E2)$ measured in units of the single-particle value $e^2\times0.02\times10^{-48}$ cm$^4$.
[b] H. E. Gove and C. Broude (Chalk River); B. M. Adams, D. Eccleshall, and M. J. L. Yates (Aldermaston); I. Kh. Lemberg (Leningrad); *Reactions between Complex Nuclei: Proceedings of the Second Conference on Reactions between Complex Nuclei, May 2–4, 1960, Gatlinburg, Tennessee* (John Wiley & Sons, Inc., New York, 1960).
[c] P. H. Stelson (Oak Ridge) (private communication).
[d] C. McGowan *et al.* (Oak Ridge), reported at the Conference on Nuclear Lifetimes, Gatlinburg ,Tennessee, October 1961 (to be published).
[e] Value may be in error. H. E. Gove (private communication).

The other part of the $B(E2)$ values may either increase or decrease the values obtained by using the single-particle operators. This other part is due to other effects, like configuration interaction, which depend on the particular states involved. These effects cannot be described by single-particle operators and must be given by two- and three-particle terms in the effective operator for the pure $f_{7/2}{}^n$ configurations.

In order to have a more complete and systematic picture, it would be interesting to have also the $B(E2)$ values of $Ti^{50}$ and $Fe^{54}$ as well as an accurate measurement of the $V^{51}$ quadrupole moment. These nuclei have closed neutron shells and $f_{7/2}{}^n$ proton configurations. The $f_{7/2}{}^n$ neutron configurations are found in the Ca isotopes. It would be instructive to have $B(E2)$ values and quadrupole moments measured in the Ca isotopes.

ACKNOWLEDGMENTS

We wish to thank Professor R. Hofstadter for his support of this project and H. von Briesen and J. Brown for help with the evaluation of the data. We are grateful to Dr. Jan Oeser for aid in the data-taking and to A. Collins for his help in programming the Stanford Computation Center's Burroughs 220 computer. Part of the computing was carried out on the MIT Compton Laboratory IGP-30 computer; in this program Miss Mida Karakashian was of material aid. Hall Crannell very kindly constructed our Čerenkov counter. This work was carried out while one of us (I. T.) was visiting at Stanford University. He would like to express his sincere thanks to the staff of the Department of Physics, and in particular to Professor L. I. Schiff, for their kind hospitality.

PHYSICAL REVIEW VOLUME 128, NUMBER 2 OCTOBER 15, 1962

# Polarization of Protons from Deuteron Stripping Reactions with a Zero Orbital Angular Momentum Transfer*

A. ISOYA† AND M. J. MARRONE‡
*Sarah Mellon Scaife Radiation Laboratory, University of Pittsburgh, Pittsburgh, Pennsylvania*
(Received March 16, 1962)

Angular dependence of the polarization of protons from the $l=0$ stripping reactions, $Al^{27}(d,p)Al^{28}{}_{g.s.+1st}$ and $Si^{28}(d,p)Si^{29}{}_{g.s.}$ has been measured at a deuteron energy of 15 MeV. Polarization changes the sign at angles close to each minimum of the angular distribution, remaining the same in the angular region corresponding to each stripping peak. The magnitude of polarization is large (20 to 30%) near the angles at which the sign change takes place.

## I. INTRODUCTION

IN recent years, considerable attention has been given to polarization of the outgoing particles from the deuteron stripping reaction.[1] Study of the polarization is considered very useful for a better understanding of the stripping reaction. Two different effects are respon-

* This work was supported by the joint program of the Office of Naval Research and the Atomic Energy Commission.
† On leave from the Institute for Nuclear Study, University of Tokyo, Japan. Present address: Lawrence Radiation Laboratory, University of California, Berkeley, California.
‡ Present address: U. S. Naval Research Laboratory, Washington, D. C.
[1] For example, a fine introduction to this phenomena is found in the following article: N. Austern, "Direct Reactions; Fast Neutron Physics" (to be published).

sible for the polarization. One is due to the spin-dependent forces which act on the incident or outgoing particles directly. The other is the distortion or absorption of the incident or outgoing waves in the optical potentials of the respective channels. The second effect influences the particle spin state because absorption or distortion determines the relative weight with which the different parts of the target nucleus contribute to the outgoing particle flux. This corresponds to a favored orientation of the orbital angular momentum transferred to the target nucleus. This condition favors a particular spin direction of the captured nucleon, depending on the $j$ value of the captured nucleon in the final state and then a particular spin direction of the outgoing nucleon through the coupling of both nucleons in the projectile deuteron. As can be seen from the above description, the polarization depends on the detailed behavior of the incident deuteron and outgoing nucleon flux on the surface and the interior of the nucleus. In such a situation, transitions with no transfer of orbital angular momentum deserve special attention since the cause of the preferred orientation of spins disappears and the situation is greatly simplified.

The effect of the spin-orbit potential on the incident or outgoing waves may be interpreted as an occurrence of different depths of the potential well for different spin directions. This results in a refractive polarization pattern as is observed in nucleon-nucleus elastic scattering. In this case, polarization is expressed as proportional to the logarithmic derivative of the cross section with respect to angle. In the case of the stripping reaction of $l=0$ transfer, existence of the same relation has been argued to a crude approximation.[2]

In this paper we present the results of measurements of proton polarization in the reactions $Al^{27}(d,p)Al^{28}{}_{g.s.+1st}$ and $Si^{28}(d,p)Si^{29}{}_{g.s.}$, in which neutron capture occurs in the $2s$-shell orbit. Since the cross sections are small ($\lesssim 1$ mb/sr) except for the forward angle stripping peak, it was necessary to maximize the counting efficiency of the polarization analyzer, even though this resulted in a loss of accuracy in the measurement. In the following sections the polarimeter used in the experiment will be described, with emphasis on the evaluation of the accuracy of the polarization measurement.

## II. THE POLARIMETER

### A. Energy-Analyzing System for the Proton Beam

The polarization measurement in deuteron stripping was designed to take advantage of the existing magnetic analyzer. Singling out the desired proton group from the outgoing particles was essential to prevent the overwhelmingly strong, elastically scattered, deuteron flux from entering the polarimeter; its intensity is usually high enough to paralyze the counting system in the polarimeter, and, furthermore, it disturbs the measurement by producing high-energy protons in the polarization analyzing scatterer.

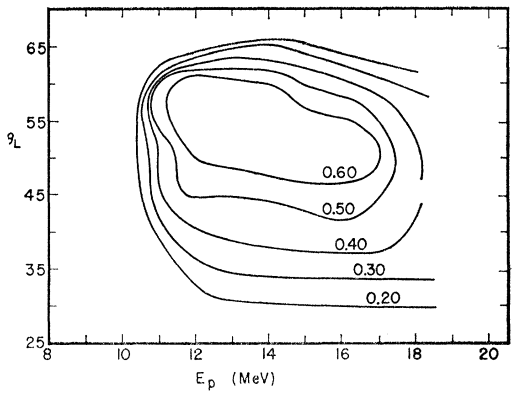


FIG. 1. Contour map of proton polarization in elastic scattering on carbon. Experimental data are taken from reference 3.

Usually the separated proton beam was contaminated by a considerable amount of deuterons, multiply scattered, especially at the forward angles (less than 10 deg). However, since the carbon scatterer in the polarimeter was thick enough to stop the deuterons, they did not disturb the measurement of scattered protons as long as the intensity of the deuterons was not more than that of the protons.

Use of the magnetic analyzer also had an advantage of reducing the $\gamma$-ray and fast-neutron background in the counters by allowing the polarimeter to be placed at some distance from the target chamber without a large reduction of the incident proton flux density.

The magnetic analyzer used was a uniform-field sector-type magnet so that its depolarization effect on the proton beam was neglected. The entrance slit of the polarimeter was placed at the focal plane of the analyzing magnet. The energy spread of the outgoing proton beam was minimized by adjusting the target angle with respect to the incident beam. For targets with a thickness of 10 to 15 mg cm$^{-2}$ the energy spread was about 200 keV. This energy spread made the focus breadth approximately as wide as the opening of the entrance slit (0.2 in.). This energy resolution was in most of the cases sufficient to resolve the proton groups from different levels of rather light nuclei.

### B. Analyzing Properties of the Polarimeter

A thinly ground graphite plate (129 mg cm$^{-2}$) was used as the analyzing scatterer in the polarimeter. Polarization of elastically scattered protons from carbon has a value of 50 to 60% in a wide energy region from 12 to 18 MeV for scattering angles around 45 deg[3] (see

[2] L. D. Biedenharn and G. R. Satchler, *Proceedings of the International Symposium on Polarization Phenomena of Nucleons, Basel, 1960* [Suppl. Helv. Phys. Acta., Suppl. VI, 1961].

[3] K. W. Brockman, Phys. Rev. **110**, 163 (1958); S. Yamabe, M. Kondo, S. Kato, T. Yamazaki, and J. Ruan, J. Phys. Soc. Japan **15**, 2159 (1960); J. Sanade, S. Suwa. I. Hayashi, K. Nisimura, N. Ryu, and H. Hasai, *Proceedings of the International*

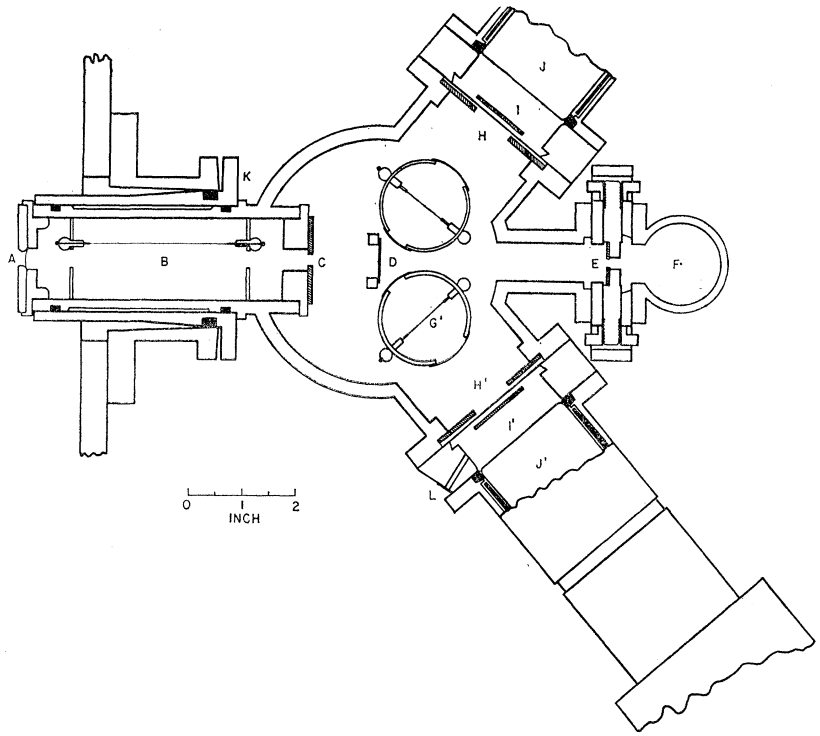


FIG. 2. Polarimeter. A, Mylar window (1 mil thick); B, gate proportional counter; C, entrance slit (0.2 in.×1 in.); D, graphite target; E, movable slit (0.2 in. wide) for the polarimeter axis alignment; F, monitor proportional counter; G, G′, proportional counter; H, H′, defining slits of the side counters; I, I′, CsI scintillators (0.8 mm thick, 1.9 in. ×1.2 in.); J, J′, photomultiplier tubes; K, polarimeter axis deflection system; L, $\alpha$-particle test window.

Fig. 1). The differential cross section is quite independent of the proton energy in this energy region. This high-polarization region covers the range of the proton energies from low-lying level formation by 15-MeV deuterons. It was therefore not necessary to adjust the proton energy before entering the polarimeter. For the same reason a very thick scatterer could be used, resulting in a high counting efficiency. However, when using the thick scatterer the inelastically scattered protons (corresponding to 4.43-MeV levels) could not be separated from the elastic group. The yield of the inelastic scattering is not small enough to be ignored and very few properties of polarization in the inelastic scattering are known. Then the procedure we adopted was to include in the counting all or some definite portion of the inelastic protons and to determine experimentally the magnitude of the effective polarization in the scattering on carbon in the actual experimental conditions. The actual procedure used in the derivation of the effective polarization value and the result will be described in the subsequent associated paper.[4]

The energy loss of the protons in the scatterer was about 4 MeV and the corresponding efficiency of the incident protons being scattered into the detector at either side of the incident beam was roughly $10^{-4}$. The mean deflection angle of protons in the scatterer was about 2 deg. This was small enough compared to the range of the scattering angles with high polarization, so no large trouble due to the broadening of the incident beam flux was expected.

### C. Detectors for the Scattered Protons

A triple-coincidence counting method was used for detection of the scattered protons in the presence of a large $\gamma$-ray background. A proportional counter (gate counter) was placed on the incident beam path in front of the entrance slit and a combination of two proportional counters or that of a proportional counter and a CsI(Tl) scintillation counter were placed on both sides of the scatterer (see Fig. 2). All the proportional counters were operated with an argon plus 5% carbon dioxide mixture at one third atmosphere which filled the whole polarimeter chamber. Background counts measured by closing the shutter in the magnetic analyzer were practically zero. In preliminary measurements a two-counter telescope was used without the gate counter, but it was found to be not enough to eliminate completely the background counts, probably caused by Compton scattering of $\gamma$ rays from counter to counter.

Scattering of the protons from argon gas made the background counts of the order of 1% of the counts of protons from the carbon scatterer, then they might be ignored.

The scattering solid angle was defined by a slit which was placed between the two counters. It ranged from 40 to 55 deg in the median scattering plane and the vertical spread was 30 deg.

*Symposium on Polarization Phenomena of Nucleons, Basil, 1960* [Suppl. Helv. Phys. Acta, Suppl. VI, 1961]; A. Strazalkowski, M. S. Bokhari, M. A. Al-Jeboori, and B. Hird, Proc. Phys. Soc. (London) **75**, 502 (1960); L. Rosen, J. Brolley, Jr., and L. Stewart, Phys. Rev. **121**, 1423 (1961).

[4] A. Isoya, S. Micheletti, and L. Reber, following paper [Phys. Rev. **128**, 806 (1962)].

The energy of the scattered protons covered a wide energy range as shown in Fig. 3. The pulse-height selector bias level for the scintillation counter output was set at the same level as the pulse height of ThC′ $\alpha$ particles which were introduced into the counter through a thin foil window for the test. This bias level was low enough to accept most of inelastic protons.

If the bias positions for the two scintillation counters in both sides are not exactly the same, an instrumental asymmetry is introduced. This was eliminated by rotating the polarimeter around the symmetry axis through 180° and calculating the asymmetry $A=(\langle R/L\rangle_{\rm av}-1)/(\langle R/L\rangle_{\rm av}+1)$ from the geometrical mean of the right and left intensity ratios measured in both positions of the polarimeter. In order to remove the effect of a possible gradual shift of the output pulse height of the scintillation counters, the rotation procedure was repeated rather frequently during a run.

As to the proportional counter, no difficulty occurred in the choice of the discriminator bias level because the lower energy particles produced the higher output pulses.

Usually a deuteron current of 1 to 2 $\mu$A was obtained on the target. Under the standard operating conditions the coincidence counting rate was 0.5 to 1 count/sec when the $(d,p)$ cross section was about 20 mb/sr. Thus, it was possible to investigate $(d,p)$ reactions with cross sections as low as 1 mb/sr with reasonable running times and statistical accuracy.

## III. INSTRUMENTAL ASYMMETRY

The instrumental asymmetry is defined as the right and left asymmetry observed when the incident beam is not polarized. It is caused by several effects. Since the interferences between the different effects are small in the actual conditions, the total instrumental asymmetry can be evaluated to a good approximation by the following formula;

$$A_{\rm instr}=A_\delta+A_\omega+A_s+A_p. \tag{3}$$

$A_\delta$ is the asymmetry due to a deviation of the polarimeter symmetry axis from the beam direction, assuming that the beam is concentrated in its center line. $A_\omega$ is the asymmetry due to a directional variation of the flux density within the finite angular spread of the beam, assuming that the incident beam is sharply focused on the scatterer and the polarimeter axis is aligned to the center of the beam. $A_s$ is the asymmetry due to the nonuniformity of the current density in the incident beam through its breadth, assuming that the beam is parallel to the polarimeter axis. $A_p$ includes all effects due to the asymmetry inherent to the polarimeter.

The polarimeter was very accurately constructed so that all the slits were placed symmetrically around the rotation axis of the polarimeter. Thus, no instrumental asymmetry was expected from geometrical causes. The rotation procedure mentioned in the last section also eliminated the possible instrumental asymmetry $A_p$, except for the effect of the external magnetic field on the scintillation counter. $A_\delta$ is given by the following formula

$$A_\delta=\frac{\sigma(40°)-\sigma(55°)}{\sigma_{\rm av}}\frac{\delta}{15}, \tag{4}$$

where $\sigma(\theta)$ is the angular distribution of the scattered protons and $\sigma_{\rm av}$ is the average of $\sigma(\theta)$ over the acceptance solid angle of the detector. $\delta$ is the misalignment angle in degrees. The magnitude of $A_\delta$ for $\delta=0.1°$ is about 0.01 in the relevant energy region.

$$A_\omega=-\frac{1}{3}\left(\frac{\partial I}{\partial\omega}\right)_0\frac{\beta}{I_0}\frac{\beta}{\theta_2-\theta_1}\frac{\sigma(\theta_2)-\sigma(\theta_1)}{\sigma_{\rm av}}, \tag{5}$$

where it is assumed that the flux density of the incident beam $I$ changes linearly as the deviation angle $\omega$ from $-\beta$ to $+\beta$. $\beta$ is determined by the window width of the magnetic analyzer and was about 0.9 deg. The change of the flux density is due to the angular distribution of the $(d,p)$ reaction being studied in the first target. The largest possible fractional change of $I$ is about 20%. Formula (5) gives the largest possible asymmetry of 0.003 for the actual conditions.

$A_s$ may be evaluated by the following formula

$$A_s=-\frac{1}{3}\left(\frac{\partial I}{\partial y}\right)_0\frac{s}{I_0}\frac{s}{R}\frac{[2\sigma\sin\theta-(d\sigma/d\theta)\cos\theta]_{\rm av}}{\sigma_{\rm av}}, \tag{6}$$

where $s$ is the half-width of the beam at the target, and $(\partial I/\partial y)_0(s/I_0)$ is a half of the fractional change of the current density from edge to edge of the beam, assuming the linear change. $R$ is the distance between the scatterer

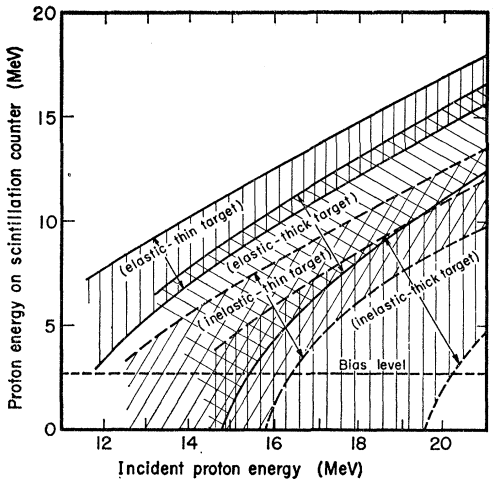


FIG. 3. Range of the scattered proton energy on the scintillation counter as a function of the incident energy to the polarimeter. Curves are shown for two different thicknesses (129 and 72 mg cm$^{-2}$) of the carbon analyzer target. Density of the distribution of the proton energy is high near the upper limits for elastic and inelastic scattering, respectively. A level position of the pulse-height selector bias determined by Th C′ $\alpha$ particles is indicated on the curve.

TABLE I. Polarization of protons from the reaction $Al^{27}(d,p)Al^{28}_{g.s.+1st}$. The first and the second columns are the reaction angles in the laboratory and the center-of-mass system, respectively. The third is the energy of protons impinging on the analyzing carbon target. The fourth is the measured asymmetry and the fifth is the effective polarization of the carbon target. The sixth is the polarization of protons from the reaction.

| $\theta_{lab}$ (deg) | $\theta_{c.m.}$ (deg) | $E_p$ (MeV) | $P_1P_2^{eff}$ | $P_2^{eff}$ | $P_1$ |
|---|---|---|---|---|---|
| 7.5 | 7.8 | 18.60 | +0.055±0.032 | −0.50 | −0.110±0.064 |
| 10.0 | 10.5 | 18.60 | −0.045±0.024 | −0.50 | +0.090±0.048 |
| 15.0 | 15.7 | 18.55 | −0.071±0.038 | −0.50 | +0.142±0.076 |
| 20.0 | 20.0 | 18.50 | −0.046±0.036 | −0.51 | +0.092±0.072 |
| 25.0 | 26.1 | 18.40 | +0.031±0.038 | −0.51 | +0.061±0.076 |
| 30.0 | 31.3 | 18.30 | +0.149±0.034 | −0.52 | −0.298±0.068 |
| 32.5 | 33.9 | 18.20 | +0.155±0.042 | −0.53 | −0.310±0.084 |
| 35.0 | 36.5 | 18.20 | +0.054±0.030 | −0.53 | −0.108±0.060 |
| 37.5 | 39.1 | 18.15 | +0.037±0.051 | −0.53 | −0.146±0.102 |
| 40.0 | 41.7 | 18.15 | +0.119±0.070 | −0.53 | −0.238±0.140 |
| 55.0 | 57.1 | 17.95 | −0.023±0.058 | −0.545 | +0.046±0.116 |
| 60.0 | 62.2 | 17.80 | −0.104±0.061 | −0.55 | +0.208±0.122 |
| 70.0 | 72.4 | 17.55 | −0.192±0.081 | −0.555 | −0.384±0.162 |

and the detector slit. The above formula takes into account the effects of change of the acceptance solid angle and the scattering angle due to the change of the beam position on the target. Assuming a fractional change of current density as 20%, formula (6) gives an asymmetry of 0.005.

The above estimation shows that in order to reduce the instrumental asymmetry less than 1% it is necessary to keep the fractional change of the incident beam current density less than about 20% and to align the polarimeter axis with accuracy better than 0.1 deg. The first requirement was fulfilled by adjusting the magnetic field of the particle analyzer to give the maximum proton beam current to the polarimeter. For measuring the beam intensity a proportional counter (monitor) was placed on the polarimeter axis behind the scatterer (see Fig. 2). During the beam alignment process the scatterer was removed from the beam path. Usually the beam current density at the entrance slit was quite uniform over the beam breadth or at least quite symmetric around the beam center axis.

For the second requirement a movable slit was placed in front of the monitor counter. By turning the polarimeter about a vertical axis in front of the entrance slit, the polarimeter axis was adjusted so that the same monitor counting rates were obtained when the slit aperture was displaced equal distances right and left. This method was sensitive enough to allow an adjustment of 0.05 deg. This alignment process located some weighted mean direction in the incident beam flux instead of the center line of the beam. Thus, the over-all asymmetry is expected to be reduced from the above estimate owing to the cancellation between $A_\delta$ and $A_\omega+A_s$. The polarimeter axis direction was readjusted whenever the reaction angle was changed because the weighted mean direction changed from angle to angle. Through the whole angular range studied the change of the polarimeter axis direction was 0.2 deg.

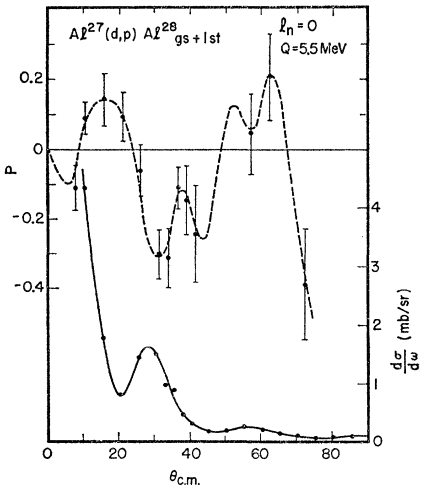


FIG. 4. Polarization of protons from the reaction $Al^{27}(d,p)Al^{28}_{g.s.+1st}$ as a function of angle. The angular distribution of the differential cross section which was obtained in the present work is also plotted. A broken line along the experimental points is drawn based on an interpretation which is discussed in the text.

## IV. MEASUREMENTS AND RESULTS; $Al^{27}(d,p)Al^{28}_{g.s.+1st}$ AND $Si^{28}(d,p)Si^{29}_{g.s.}$

The $l=0$ transfer in all three transitions studied has been established by the angular distribution measurements.[5,6] $Q$ values in these transitions are roughly the same. The proton groups for the two lowest close levels of $Al^{28}$ were studied together because the separation of these groups was impossible (energy spacing is 31 keV). An aluminum foil of 2 mils and a silicon crystal uniformly ground in the thickness of 14.3 mg cm$^{-2}$ were bombarded by the 15-MeV energy-analyzed deuteron beam. The actual energy loss of the deuterons in the target was 600 to 800 keV depending on the target angle. The energy of protons emitted forward from the target was 18.7 and 19.6 MeV, respectively, in the

TABLE II. Polarization of protons from the reaction $Si^{28}(d,p)Si^{29}_{g.s.}$.

| $\theta_{lab}$ (deg) | $\theta_{c.m.}$ (deg) | $E_p$ (MeV) | $P_1P_2^{eff}$ | $P_2^{eff}$ | $P_1$ |
|---|---|---|---|---|---|
| 7.5 | 7.8 | 19.40 | −0.004±0.046 | −0.40 | +0.010±0.120 |
| 10.0 | 10.4 | 19.40 | −0.009±0.028 | −0.40 | +0.023±0.070 |
| 12.5 | 13.0 | 19.28 | −0.044±0.030 | −0.40 | +0.110±0.075 |
| 14.0 | 14.5 | 19.27 | −0.031±0.033 | −0.40 | +0.078±0.083 |
| 17.5 | 18.2 | 19.20 | −0.061±0.042 | −0.40 | +0.153±0.110 |
| 20.0 | 20.8 | 19.15 | −0.088±0.072 | −0.41 | +0.215±0.180 |
| 25.0 | 26.0 | 19.05 | +0.096±0.043 | −0.43 | −0.223±0.100 |
| 30.0 | 30.7 | 19.10 | +0.018±0.037 | −0.42 | −0.043±0.086 |
| 35.0 | 36.3 | 19.05 | +0.049±0.044 | −0.43 | −0.114±0.100 |
| 40.0 | 41.5 | 19.05 | +0.060±0.059 | −0.43 | −0.140±0.140 |
| 45.0 | 46.6 | 18.90 | +0.117±0.098 | −0.46 | −0.257±0.200 |
| 55.0 | 56.9 | 18.70 | −0.100±0.059 | −0.48 | +0.208±0.123 |
| 60.8 | 62.0 | 18.60 | −0.012±0.059 | −0.50 | +0.024±0.119 |
| 70.8 | 72.2 | 18.35 | −0.004±0.066 | −0.52 | +0.007±0.130 |

[5] M. H. Macfarlane and J. B. French, Revs. Modern Phys. **32**, 567 (1960).

[6] A. Blair, Ph.D. thesis, University of Pittsburgh, 1960 (unpublished).

reactions. Since these values were a little too high to be admitted into the polarimeter, their energies were reduced by about 1 MeV using a Mylar absorber which was placed close to the target on the outgoing path. The effective polarization of the carbon analyzer was obtained from the curve in Fig. 1 in the associated paper.[4] The results of the measurements are shown in Tables I and II. The sign of the polarization is chosen to be positive when the polarization vector is in the direction of $\mathbf{k}_d \times \mathbf{k}_p$. Errors listed include only the statistical errors. The error due to the uncertainty of the $P_2^{\text{eff}}$ value is about 10% of the measured value and the systematic error due to the instrumental asymmetry is $\pm 0.02$, at most.

The angular dependence of the polarizations are plotted in Figs. 4 and 5, together with the angular distributions of the cross sections.

## V. DISCUSSION

The two polarization angular dependence curves obtained from the measurement are very similar. The correspondence between the polarization and the cross-section curves seems to be almost unique. The cross section for aluminum at higher angles varies a little more rapidly than for silicon, as is predicted from the difference of $Q$ values of 0.75 MeV by the plane-wave stripping theory. Correspondingly, the polarization pattern for the former is considered to have a more rapid cycle than for the latter. A remarkable feature of the observed curves is that the polarization sign changes at angles close to each minimum of the angular distribution, remaining the same in the angular region corresponding to each stripping peak. Swing of the polarization value at the minimum points is so rapid that the shape of the polarization curve looks like a refraction pattern. However, the derivative rule, mentioned in the introduction, is not generally verified because the sign does not change at every stationary point of the angular distribution curve as required by this rule. The sign change of the polarization seems to be connected to the sign change of the stripping amplitude. Such a property of the polarization angular dependence has been mentioned by Newns *et al.*[7] to explain the feature of the calculated polarization curve for the reaction $C^{12}(d,p)C^{13}$.

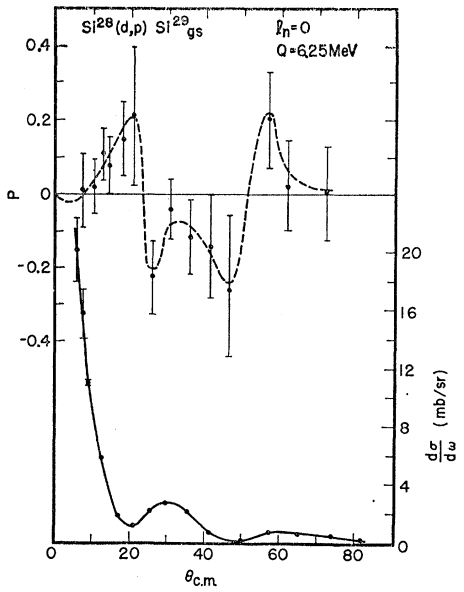


FIG. 5. Polarization of protons from the reaction $Si^{28}(d,p)Si^{29}_{g.s.}$ as a function of angle. The angular distribution of the differential cross section, taken from reference 6, is also plotted. A dashed line along the experimental points is drawn based on an interpretation which is discussed in the text.

## ACKNOWLEDGMENTS

We wish to express our sincere thanks to Professor A. J. Allen, Professor D. Halliday, and Professor B. L. Cohen for support and encouragement. We are also grateful to Professor N. Austern, Dr. G. R. Satchler, Professor K. Quisenberry, and Dr. E. Hamburger for helpful discussions and advice. We owe very much to Dr. S. Micheletti, L. Reber, T. Kuo, and the cyclotron laboratory staff for assistance in this work.

[7] H. C. Newns and M. Y. Refai, Proc. Phys. Soc. (London) **A71**, 627 (1958).